Accepted Manuscript

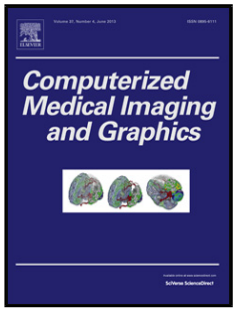

Title: Automatic Rectum Limit Detection by Anatomical Markers Correlation

Author: R. Namías J.P. D'Amato M. del Fresno M. Vénere

PII: S0895-6111(14)00015-9
DOI: http://dx.doi.org/doi:10.1016/j.compmedimag.2014.01.005
Reference: CMIG 1239

To appear in: *Computerized Medical Imaging and Graphics*

Received date: 3-5-2013
Revised date: 19-12-2013
Accepted date: 23-1-2014

Please cite this article as: R. Namías, J.P. D'Amato, M. del Fresno, M. Vénere, Automatic Rectum Limit Detection by Anatomical Markers Correlation, *Computerized Medical Imaging and Graphics* (2014), http://dx.doi.org/10.1016/j.compmedimag.2014.01.005

Automatic Rectum Limit Detection by Anatomical Markers Correlation

R. Namías[a,c], J. P. D'Amato[b,c], M. del Fresno[b,d], M. Vénere[b,e]

[a] *CIFASIS, Centre Internacional Franc-Argentin de Sciences de l'Information et de Systmes, UAM (France) / UNR-CONICET, Rosario, Santa Fe, Argentina,*
[b] *Instituto PLADEMA, Universidad Nacional del Centro, Tandil, Argentina*
[c] *Consejo Nacional de Investigaciones Científicas y Técnicas (CONICET), Argentina*
[d] *Comisión de Investigaciones Científicas de la Prov. de Buenos Aires (CIC-PBA), Argentina*
[e] *Comisión Nacional de Energía Atómica (CNEA), Argentina*

Abstract

Several diseases take place at the end of the digestive system. Many of them can be diagnosed by means of different medical imaging modalities together with computer aided detection (CAD) systems. These CAD systems mainly focus on the complete segmentation of the digestive tube. However, the detection of limits between different sections could provide important information to these systems.

In this paper we present an automatic method for detecting the rectum and sigmoid colon limit using a novel global curvature analysis over the centerline of the segmented digestive tube in different imaging modalities. The results are compared with the gold standard rectum upper limit through a validation scheme comprising two different anatomical markers: the third sacral vertebra and the average rectum length. Experimental results in both Magnetic Resonance Imaging (MRI) and Computed Tomography Colonography (CTC) acquisitions show the efficacy of the proposed strategy in automatic detection of rectum limits. The method is intended for application to the rectum segmentation in MRI for geometrical modeling and as contextual information source in virtual colonoscopies and CAD systems.

Keywords: Anatomical Markers, Colon, Rectum, Computed Tomography, Magnetic Resonance Imaging.

1. Introduction

The lower section of the digestive tube is composed of the colon sigmoid, the rectum and the anus, where several diseases take place. Particularly in the rectum, the most common conditions are partial or complete prolapse and cancer (carcinoma) [1, Ch. 7]. New imaging protocols have recently stood out as common techniques for helping clinicians in the better diagnosis of these illnesses. On the one hand, CTC is a 3D medical imaging technique that produced a great impact in colorectal cancer (CRC) diagnosis. Actually, the CRC screening tests are grouped into cancer prevention tests and cancer detection tests according to the American College of Gastroenterology [2]. On the other hand, MRI and CT have gained acceptance and reliability in the diagnosis of pelvic organ prolapse thanks to research carried out in the last few years [3, 4, 5].

Computer aided detection systems started to play an important role in clinical diagnosis. CAD systems were developed in a wide array of medical areas such as cardiology, ophthalmology, dermatology, gynecology, oncology, gastroenterology, etc. In the last decade, many CAD and diagnosis systems have been proposed and actively studied to improve the performance and reliability of human radiologists as second readers [6]. Although there are yet no CAD systems for pelvic organ prolapse, several ones were proposed for colon cancer diagnose in CTCs [7, 8, 9]. In their beginnings, the CAD systems for CTC studies were proved to play an important complementary role to trained specialists in polyps detections [10]. The continue development of these system helped to reduce the variability among readers [11] and the inspection time

Email address: namias@cifasis-conicet.gov.ar (R. Namías)

needed by the specialists [12]. Nowadays they have an epidemiology importance for polyps cancer diagnosis [13]. These systems automatically segment the colon in CTC [14, 15], determine the locations of suspicious polyps and masses and present them to radiologists, typically as a second opinion having a clinically acceptable high sensitivity and a low false-positive rate [16].

Although the well-known relevance of the CAD systems for CTCs, no extra efforts were done to automatically add contextual information to these systems. To the best of our knowledge, extra semantic analysis were made by *Hu et all* [17] to divide lower digestive tube on its base segments in CTC using user-provided points of reference. However, this semi-automatic method needs several anatomical markers points to complete the division of the digestive tube parts. It comprehends a quite complex method of several stages to achieve its goal.

Addressing contextual information in CAD systems for the colorectal cancer detection is an important application of the proposed method. However, it can also be used in the pelvic prolapse evaluation. Volumetric geometrical models are used to simulate the dynamics of the main pelvic organs (bladder, rectum, uterus) during an abdominal muscle strain to evaluate the organ prolapse [18]. For this purpose, firstly it is necessary to accurately segment these organs from MRI volumetric acquisitions. Determining the exact rectum limit is essential for this task giving an extra importance to this method.

In this paper we present a new procedure for the automatic detection of the upper rectum limit. The method is based on the centerline curvature analysis of the segmentation obtained from the lower digestive tube. It improves the existing previous work as it does not require the user intervention and it can be applied in different imaging modalities. Hence, it could easily be incorporated in many actual CAD systems and segmentation tasks.

In the next section we describe the medical data, outlining a brief description of the state-of-art segmentation techniques and centerline extraction employed for CTC acquisitions and the chosen method used in this work. Next, in section 3 we first present an extensive curvature feature analysis of the centerline leading to the rectum limit detection method. Experimental results in both CTCs and pelvic volumetric MRIs acquisitions are evaluated with the ground truth given by the specialists. We also pose an evaluation of a correlation between the obtained limits and the most important anatomical marker commonly used by the specialists using an ad-hoc validation procedure. Finally, we summarize the experimental results and direct future work.

2. Materials and Methods

2.1. Medical Data

Unlike other works, we try to generalize a procedure to find the rectum's upper limit by considering studies from two different volumetric imaging modalities: CTC and MRI.

The CTC colonography collection was downloaded from the National Cancer Institute's Image Cancer Archive (http://cancerimagingarchive.net/) whereas the MRI acquisitions come from patients from La Timone hospital in Marsille, France. The CTC scans were made by an helicoidal TOSHIBA CT using a 120 kVp protocol. The studies have between 340 and 588 slices, with a 512x512 pixel resolution and a $[0.702, 0.702, 0.800]mm$ average spatial resolution with an Axial-LPI orientation.
The MRI scans are under a T2 weighted FSE Sagittal protocol, having 110 slices with a 256x256 pixel resolution and a $[0.781, 0.781, 1.00]mm$ average spatial resolution.

2.2. Segmentation

For colon segmentation in CTC acquisitions, numerous automatic techniques were proposed in the literature [14, 19, 20]. These techniques are all mainly based on a region growing process with an automatic seed detection and a post processing stage to improve the lumen segmentation which can sometimes may be obstructed by peristalsis, large masses, and/or residual feces. However, these methods are not so useful for the segmentation of the same organs on MRI images because of dissimilar images characteristics.

For the final work purpose, we use a more favorable method that could deal with both sorts of studies. It consist in a variation of the hybrid active surface method presented in [21] which has been improved with an algorithm for self-collide detection (SCD) to avoid mesh artifacts during its evolution. The resulting method consists on three main stages. First, a manually seeded region growing (RG) technique is applied to obtain an initial organ segmentation. In the second stage, we convert the RG output

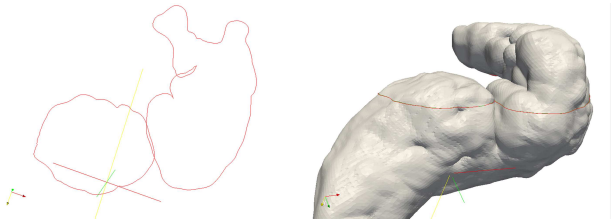

Figure 1: Mesh with self-intersecting elements. (left) 2D Plane cut where surface is overlapping (right) 3D mesh view.

into a triangular 3D surface mesh. As the resulting mesh has "staircase" artifacts, it can be smoothed using a Taubin filter, described in [22]. In this third and last stage, we employ a variation of an active surface algorithm with (SCD) which provides the final mesh.

2.2.1. Robust Active Surface Model

The active surface model, called T-Surface by Mcinerney et al. [23], is used to gather a subvoxel precision segmentation of complex-shaped structures from medical images. However, when this technique is applied on self-folding organs, several artifacts can show up, as inverted o collapsing triangles as shows Figure 1, that make the mesh unsuitable for calculus.
In order to avoid these topological problems we employ the SCD scheme to detect triangles collisions or self-intersections.

The evolution algorithm starts with a collision-free state coming from the RG method, which provides a suitable snake initialization. The model evolves under the influence of internal and external forces, and collisions are checked every a given number of deformation steps. As all-to-all triangle collision test is very expensive, elements should be classified to test only potential collisions. This test is made as follows:

1. Triangles are projected over a grid in the $xy-plane$.
2. For every non-empty cell of the grid, all triangles in this cell are tested. If collision occurs, the two triangles are added to a list.
3. Return the list of collided triangles.

If the list is empty, it means that the current state of the snake model is collision-free and the evolution can continue. If not, we do a *rollback* of the whole mesh to the previous checkpoint, freeze the nodes which were involved in the collision and continue evolving. A complete mesh rollback is necessary due to the node neighbor dependance in two of the model forces forces. This procedure ensures that meshes are free from inverted elements in every evolution step.

2.3. Anatomical Markers

Organs section discrimination is usually based on spatial observation rules, as "is in front of" or "is behind" a distinguishable part of the body. As we want to delimit the rectum, here we propose to use the same methodology as the experts. When they look for the rectum upper limit, they directly search the S3 anatomical marker, as in [17] for the correlation analysis with the curvature analysis. Therefore, we manually segmented the S3 vertebra using the ITK-SNAP (www.itksnap.org) toolkit.

2.4. Skeletonization

One efficient way to determine the physiognomy of the organ is by extracting what is called the skeleton or centerline. This is a simple way to identify foldings or bends along the studied organ. The skeletonization process is done after the segmentation step. Despite several works directly skeletonize from the voxel mask [24, 25], as our segmentation result is a surface mesh, we employ the *Dijkstra's skeleton algorithm*[26] which was used in different works, such as *Lu et al.* [20]. This algorithm is widely used in virtual colonoscopies, proved to be reasonable for our purpose and was visually validated by the expert.

2.5. Curvature Analysis

The skeletonization output is a group of ordered points $\{p_s^i\}$ which describes a polygon in space. We need to determine whether or not there is a correlation between the bottom digestive tube curves and the S3 anatomical marker. The S3 vertebra is important because points out the end of the rectum and the beginning of the sigmoid colon.
We propose and study three different approaches for measuring curvature along the tube skeleton: Splines Curvature (SC), Global Splines Curvature (GSC) and Line Mean Differences Curvature (LMDC). Next, we briefly describe each technique and compare their results for the final purpose of detecting the actual curves of the colon.

2.5.1. Splines Curvature

The first curvature analysis approach consists in the differential geometry curvature definition of any

parametric curve $\Gamma(t)$. Given a parametric representation of a curve in space, $\Gamma(t) : \mathbf{R} \rightarrow \mathbf{R}^3$; the curvature $\kappa(t)$ is defined as:

$$\kappa(t) = \frac{\|\Gamma(t)' \times \Gamma(t)''\|}{\|\Gamma(t)'\|^3} \quad (1)$$

Therefore, for the sake of measuring this magnitude, we computed by interpolation an an extended Catmull-Rom cubic spline passing through the skeleton points $\{p_s^i\}$. As shows [27], is really straightforward to calculate the polynomials and their analytics first and second order derivatives. Hence, we calculate the curvature $\kappa(t)$ over any interpolated point in the spline.

2.5.2. Global Splines Curvature

With the purpose of achieving a more macroscopic notion of curvature we propose, instead of computing the κ curvature value for each interpolated point of the spline, to use an odd length sliding window (W_k) over the skeleton points defining a new $\kappa(W_k)$ curvature as:

$$\kappa(W_k) = \left\| \frac{1}{\#(W_k)} \sum_{t \in W_k} \left(\frac{\Gamma(t)' \times \Gamma(t)''}{\|\Gamma(t)'\|} \right) \right\| \quad (2)$$

where k is the window length, $\#(W_k)$ is the amount of interpolated samples in the current sliding window. This new metric have a couple of important issues. First, it is calculated only on each of the p_k points, second it measures the module of the average curvature direction over the spline samples that belongs to W_k and assigns it to the W_k middle point. In this way, we are obtaining a more global curvature feature.

2.5.3. Line Mean Difference Curvature

The final approach is radically different from the previous two; it is based on an even more intuitive notion of curvature. We take again an odd length sliding window (W_k) over the skeleton points as in the GPC. Then, a *supporting line* (SL) is sketched among the first and the last point of the window. For all the inner points of the window we obtain the analytic projection over the SL gathering $k-2$ displacement vectors (Figure 2 shows an example). Next, we average these displacement vectors obtaining the mean difference vector (mdv) from the SL and finally we assign the mean difference vector module to the W_k middle point.

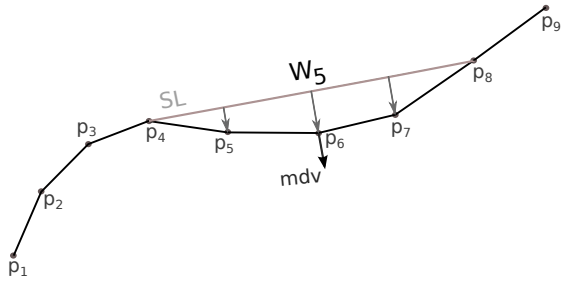

Figure 2: A W_5 sliding window centered in p_6; SL sketched among p_4 and p_8; the 3 displacement vectors between the SL and the inner points $\{p_5, p_6, p_7\}$; and the mean difference vector below p_6.

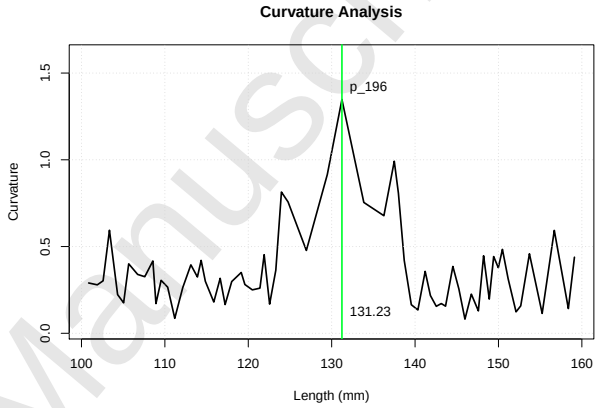

Figure 3: LMDC among the skeleton RI. In green depicted the maximum value (p_s^{196}) 131.23mm away from the end of the rectum.

2.6. Rectum Limit Detection

We propose to find the limit of the rectum by analyzing the curvature magnitude among the skeleton. The lower digestive tube could measure more than one meter, having several folds. Therefore, using the skeleton points $\{p_s^i\}$ in the original spatial coordinates provided by the DICOM standard we can approximate the path length of the skeleton in millimeters (mm) by adding each skeleton segment length. So, we first restrict the complete interval to the rectum interval (RI) which is the average rectum length $130 \pm 30mm$. Along these line, now we define the limit of the rectum as the point $p_s^i \in RI$ where its curvature is maximum (see Figure 3).

3. Experimental Results

In this section we validate the proposed method. First, we describe the anatomical marker validation scheme based on an accepted methodology from specialists. Second, we examine the optimal window size

parameter of the different curvature analysis. Next, we compare the accuracy of the algorithm variations measuring the error rate. Finally we confirm the correlation hypothesis between the method results and the anatomical marker validation scheme.

3.1. Anatomical Marker Validation Procedure

The anatomy books outline that the rectum begins in front of the S3 [1]. Therefore, we analyze the obtained limit point within a region in front of the S3. In order to do that, we place a plane over and below the manually segmented S3 mesh and get its intersection with the skeleton. We name the intersection interval as the *S3 point interval* (S3-PI). Then, we check if the limit point resulting from the curvature analysis is within the S3-PI interval. In Figure 4 we show the validation scheme to evaluate the proposed method .

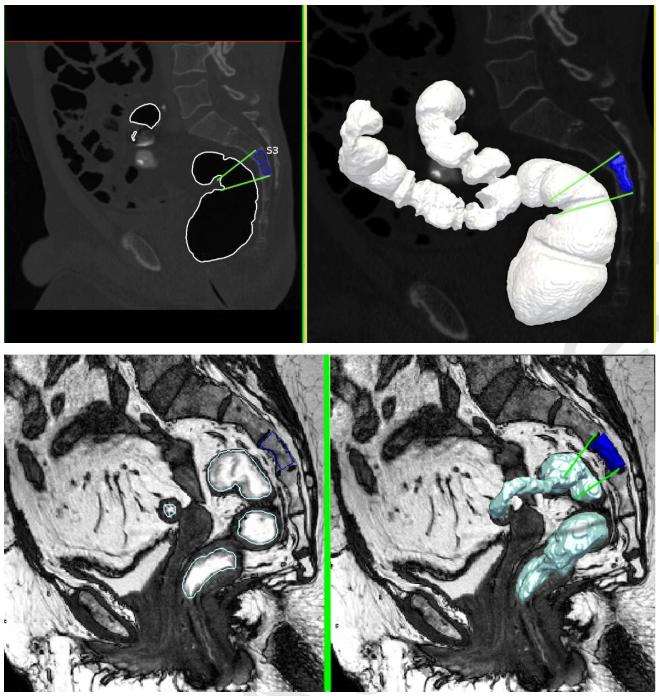

Figure 4: Anatomical Marker Validation Scheme in CTC and MRI images. S3 limits are projected over the digestive tube to determine a valid limit interval. On the left of each modality, a 2D slide projection of the S3 limits over the digestive tube border. The right sides show the corresponding 3D visualization.

3.2. Window Size Sensibility

Considering the ground truth limits given by a specialist, we examined the sensibility and the optimum values for the window size parameters in the proposed curvature methods. We considered all the acquisitions in both modalities. For the experiments we take as error, the distance between the limit point marked by the specialist over the skeleton versus the curvature results given by the methods. For SC, we just show the error distribution over the different studies. For LMDC and GSC we did the same varying the window size between $5mm$ and $65mm$.

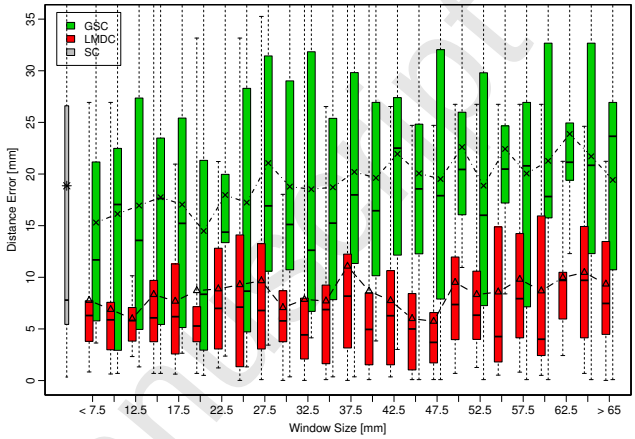

Figure 5: Methods error distributions changing the windows size parameter. In grey the SC (no window), in green the GSC and in red the LMDC. In dashed line the mean error of each method.

Figure 5 summarizes the experiments results. In the x-axis the window size intervals and in the y-axis the error of the method. We see that the best method is the LMDC using a window size between $10mm$ and $12.5mm$. It presents the lowest mean error but not the lowest median error value. Nevertheless, it works well for every case, having the lowest variability and closest outliers. In the same way, the GSC method performs better using a window size within $20mm$. These windows sizes were used in the following analysis.

3.3. Method Comparison

Figure 6 compares the different curvature methods. The resulting error distances given by each method were sorted and presented as an accumulative distribution. In this way, we can see that the LMDC outperforms the other two curvature analysis. All their results are below $11mm$ of the results given by the specialist. For the other two, $20mm$ are necessary to reach about an 80% of accuracy.

3.4. Anatomical Markers Correlation Analysis

As we described before, the method was applied to two different real image modalities. The first group

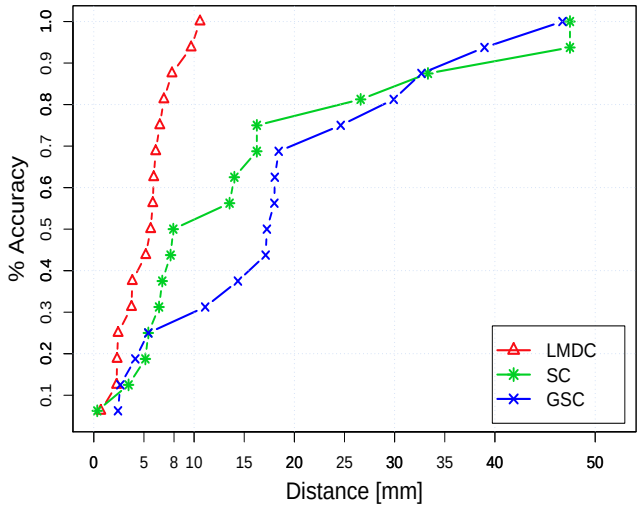

Figure 6: ROC-like curve. In the x-axis the distance error committed by the different methods. In the y-axis the accumulated accuracy comprehended in the distance interval.

consists in a CTC image pack of five patients where there are more than one acquisition for each patient. The second group comprises rectum contrast enhanced ultrafast T2 weighted spin-echo MRIs acquisitions from other four different patients.

The experiments shown in Table 1 depict that the limit points gathered by the proposed curvature analysis are within the S3-PI in almost every study. As well, the rectum length matches the RI. For the patient 86 CTC studies† have their first acquired axial plane over the rectum ending. For this reason, the obtained length is nearby the lower RI limit.
In addition, the 19_1 study was the only case that did not pass the validation. In particular, the centerline returned by the *Dijkstra's skeleton algorithm* did not fit accurately to the organ mesh, causing the analysis to displace the rectum limit. Moreover, Table 1 corroborates the correlation between the curvature analysis results and the common methodology based on anatomical markers used by the specialists.

The whole process (since RG to organs separation) needs about 4-5 minutes in a personal computer, the curvature analysis is instantaneous ($< 1sec$) what shows to be useful in a as a routinary analysis. In addition, the analysis of the digestive tube curvature is independent from the medical modality because is based on the human anatomy. Having an appropriate segmentation and organ centerline we can apply the method as shows the experiments.

Application example. In Figure 7 we present an application example of the rectum limit detection method.

Patient	Total Length	S3-PI	LMDC Limit	Real Limit	
19_0	676.44	[113.63-140.85]	125.67	121.91	✓
19_1	355.21	[142.80-163.95]	140.77	143.10	x
19_2	215.46	[121.53-146.11]	125.99	133.78	✓
20_0	676.44	[113.63-140.85]	125.67	123.248	✓
20_1	1704.72	[84.96-114.81]	108.59	106.315	✓
20_2	575.48	[104.60-127.87]	125.69	119.81	✓
86_0	1808.92	[78.28-111.11]	106.56†	95.97	✓
86_1	1775.82	[95.06-122.95]	101.86†	102.55	✓
173_1	497.19	[129.15-152.04]	151.05	144.88	✓
173_2	268.48	[112.54-142.54]	131.23	121.53	✓
174_0	1177.34	[90.27-128.85]	106.14	111.81	✓
174_1	678.70	[81.44-127.66]	122.77	100.47	✓
14	154.37	[105.88-128.17]	114.98	120.16	✓
16	155.08	[93.85-118.14]	114.01	107.43	✓
27	137.93	[85.16-112.15]	110.01	106.17	✓
39	305.26	[102.06-127.08]	108.86	114.83	✓

Table 1: summarizes the rectum limit detection experiments. The two image groups are divided by an horizontal line. The first group corresponds to CTCs and the second one to MRIs. The second column represent the total length of the digestive tube, in millimeters. The third one is the interval (S3-PI) retrieved by the procedure described in section 3.1. The two last column exhibits the rectum limit in millimeters gathered with the LMDC curvature analysis and finally the real limit marked by the specialist.

We show two rectum segmentations one for each imaging modality. In order to find the organs boundaries in the segmented region, we place a plane perpendicularly to the centerline in the limit point found by the proposed method. This plane cuts the surface mesh giving actual ending border of the rectum.

4. Discussion and conclusion

We have presented a method to automatically determine the rectum upper limit in two different types of 3D medical images. The method uses a fast curvature analysis of the segmented organ skeleton based on well-known anatomical markers: relative position and length. The quantitative experiments show that the LMDC technique overcomes the other two approaches. In addition, the results showed a high correlation with the proposed anatomical marker validation procedure that resembles the methodology used by the specialists. Finally, a segmentation example was presented as a possible application of the proposed method to rectum segmentation task for prolapse diagnosis.
In future works, we will extend the analysis to the whole colon in order to get the limits of other colon

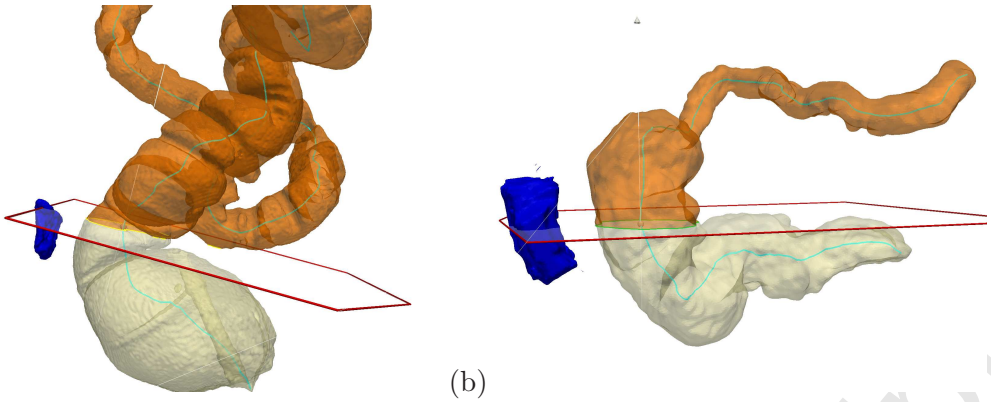

(a) (b)

Figure 7: Rectum segmentation examples using the gathered limits: (a) CTC - Patient 20_1. (b) MRI - Patient 39.

segments. It may be interesting to apply the method in CTC studies and virtual colonoscopies without further processing or in segmentation tasks.

References

[1] R. S. Snell, Clinical Anatomy by Regions, ninth Edition, Lippincott Williams & Wilkins, 2012, Ch. 7, pp. 766–774.

[2] D. Rex, D. Johnson, J. Anderson, P. Schoenfeld, C. Burke, J. Inadomi, American college of gastroenterology guidelines for colorectal cancer screening 2008, American Journal of Gastroenterology 104 (3) (2009) 739–750.

[3] N. Okamoto, K. Maeda, R. Kato, S. Senga, H. Sato, R. Hosono, Dynamic pelvic three-dimensional computed tomography for investigation of pelvic abnormalities in patients with rectocele and rectal prolapse, Journal of Gastroenterology 41 (8) (2006) 802–806.

[4] H. Pannu, Magnetic resonance imaging of pelvic organ prolapse, Abdominal Imaging 27 (6) (2002) 660–673.

[5] L. Berman, G. Israel, S. McCarthy, J. Weinreb, W. Longo, Utility of magnetic resonance imaging in anorectal disease, World Journal of Gastroenterology 13 (23) (2007) 3153–3158.

[6] M. Giger, H.-P. Chan, J. Boone, Anniversary paper: History and status of cad and quantitative image analysis: The role of medical physics and aapm, Medical Physics 35 (12) (2008) 5799–5820.

[7] T. Chowdhury, P. Whelan, O. Ghita, The use of 3D surface fitting for robust polyp detection and classification in CT colonography, Computerized Medical Imaging and Graphics 30 (8) (2006) 427–436.

[8] L. Lu, M. Wolf, J. Liang, M. Dundar, J. Bi, M. Salganicoff, A two-level approach towards semantic colon segmentation: removing extra-colonic findings, MICCAI (2009) 1009–1016.

[9] H. Yoshida, A. Dachman, Computer-aided diagnosis for ct colonography, in: Seminars in Ultrasound, CT, and MRI, Vol. 25, Elsevier, 2004, pp. 419–431.

[10] R. M. Summers, A. K. Jerebko, M. Franaszek, J. D. Malley, C. D. Johnson, Colonic polyps: Complementary role of computer-aided detection in ct colonography1, Radiology 225 (2) (2002) 391–399.

[11] H. Yoshida, A. H. Dachman, Computer-aided diagnosis for ct colonography, Seminars in Ultrasound, CT and MRI 25 (5) (2004) 419 – 431.

[12] H. Yoshida, J. Näppi, Three-dimensional computer-aided diagnosis scheme for detection of colonic polyps, Medical Imaging, IEEE Transactions on 20 (12) (2001) 1261–1274.

[13] L. Bogoni, P. Cathier, M. Dundar, A. Jerebko, S. Lakare, J. Liang, S. Periaswamy, M. E. Baker, M. Macari, Computer-aided detection (cad) for ct colonography: a tool to address a growing need, British Journal of Radiology 78 (suppl 1) (2005) S57–S62. doi:10.1259/bjr/25777270.

[14] C. Wyatt, Y. Ge, D. Vining, Automatic segmentation of the colon for virtual colonoscopy, Computerized Medical Imaging and Graphics 4 (1) (2000) 1–9.

[15] G. Slabaugh, X. Yang, X. Ye, R. Boyes, G. Beddoe, A robust and fast system for ctc computer-aided detection of colorectal lesions, Algorithms 3 (1) (2010) 21–43. doi:10.3390/a3010021.
URL http://www.mdpi.com/1999-4893/3/1/21

[16] H. Yoshida, J. Näppi, Cad in ct colonography without and with oral contrast agents: Progress and challenges, Computerized Medical Imaging and Graphics 31 (4-5) (2007) 267–284, cited By (since 1996)28.

[17] Y. Hu, M. S. Ahamed, E. Takahashi, H. Suzuki, Y. Kawata, N. Niki, M. Suzuki, G. Iinuma, N. Moriyama, Segmentation algorithm of colon based on multi-slice ct colonography (2012) 831438–9.

[18] T. Bay, J. Chambelland, R. Raffin, M. Daniel, M. Bellemare, Geometric modeling of pelvic organs, in: Engineering in Medicine and Biology Society, EMBC, 2011 Annual International Conference of the IEEE, IEEE, 2011, pp. 4329–4332.

[19] A. Bert, I. Dmitriev, S. Agliozzo, N. Pietrosemoli, M. Mandelkern, T. Gallo, D. Regge, An automatic method for colon segmentation in CT colonography, Computerized Medical Imaging and Graphics 33 (4) (2009) 325–331.

[20] L. Lu, J. Zhao, An improved method of automatic colon segmentation for virtual colon unfolding, Computer Methods and Programs in Biomedicine 109 (1) (2013) 1–12.

[21] M. del Fresno, M. Vénere, A. Clausse, A combined region growing and deformable model method for extraction of closed surfaces in 3D CT and MRI scans, Computerized Medical Imaging and Graphics 33 (5) (2009) 369–376.

[22] G. Taubin, A Signal Processing Approach to Fair Sur-

face Design, Computer Graphics 29 (Annual Conference Series) (1995) 351–358.
[23] T. Mcinerney, D. Terzopoulos, Topology adaptive deformable surfaces for medical image volume segmentation, IEEE Transactions on Medical Imaging 18 (1999) 840–850.
[24] R. J. Sadleir, P. F. Whelan, Fast colon centreline calculation using optimised 3D topological thinning, Computerized Medical Imaging and Graphics 29 (4) (2005) 251 – 258.
[25] C. Arcelli, G. Sanniti Di Baja, L. Serino, Distance-driven skeletonization in voxel images, IEEE Transactions on Pattern Analysis and Machine Intelligence 33 (4) (2011) 709–720.
[26] Y. Samara, M. Fiebich, A. Dachman, J. Kuniyoshi, K. Doi, K. Hoffmann, Automated calculation of the centerline of the human colon on CT images, Academic Radiology 6 (6) (1999) 352–359.
[27] E. Catmull, R. Rom, A class of local interpolating splines, Computer aided geometric design. Academic Press. (1974) 317–326.

Rafael Namias received his B.S. degree in Computer Science from Rosario National University, Rosario, Argentina, in 2007. He is currently a Ph.D. Candidate in Centro Internacional Franco Argentino de Ciencias de la Información y Sistemas (CIFASIS). His research interests are in the areas of medical imaging, segmentation, and features analysis.

Juan Pablo D'Amato is Phd in Computational and Industrial Mathematics since 2011 at the UNICEN University (Tandil, Argentina). Hes professor assistant in Computer Graphics courses and has worked in the development of real time systems and simulators for the Argentine Army Forces. His main research interests include geometry, high performance in GPUs, visualization and virtual reality applied to training.

Mariana del Fresno received her PhD (2008) at the UNICEN University (Tandil, Argentina). Currently she is professor in the Department of Computer Science at the same University and member of the Comisión de Investigaciones Científicas de la Provincia de Buenos Aires. Her research interests include medical image processing, segmentation and visualization.

Marcelo Vénere is a PhD in Nuclear Engineering from Balseiro Institute, Argentina. Hes an Associated Professor in Computer Graphics and Algorithms courses at the UNICEN University (Tandil, Argentina). He is leading several projects in arterial fluid simulation, real time training and computer graphics; among other topics. He is the Co-Director of the PLADEMA Research Institute of the UNICEN University at Tandil, Argentina.